Determination of the Secondary Structure and Conformation of Puroindolines by Infrared and Raman Spectroscopy †

5 AUTHORS, INCLUDING:

Thierry Le Bihan
The University of Edinburgh
50 PUBLICATIONS 962 CITATIONS

SEE PROFILE

Didier Marion
French National Institute for Agricultural Res…
156 PUBLICATIONS 5,234 CITATIONS

SEE PROFILE

Determination of the Secondary Structure and Conformation of Puroindolines by Infrared and Raman Spectroscopy[†]

Thierry Le Bihan,[‡] Jean-Érik Blochet,[‡] André Désormeaux,[‡] Didier Marion,[§] and Michel Pézolet*,[‡]

*Centre de Recherche en Sciences et Ingénierie des Macromolécules, Département de chimie, Université Laval,
Cité Universitaire, Québec, Canada G1K 7P4, and Laboratoire de Biochimie et Technologie des Protéines, Institut National de
la Recherche Agronomique, Rue de la Géraudière, B.P. 1627, 316 Nantes Cedex 03, France*

ABSTRACT: The conformation of puroindoline-a and -b, two basic lipid-binding proteins isolated from wheat seedlings, has been studied for the first time by infrared and Raman spectroscopy. The infrared results show that puroindoline-a and -b have similar secondary structure composed of approximately 30% α-helices, 30% β-sheets, and 40% unordered structure at pH 7. The conformation of both puroindolines is significantly pH-dependent. The reduction of the disulfide bridges leads to a decrease of the solubility of puroindolines in water and to an increase of the β-sheet content by about 15% at the expense of the α-helix content. Raman spectroscopy confirms the structure similarity between the two puroindolines with little differences in the side chains' environment. All the disulfide bridges are in a *gauche−gauche−gauche* conformation, and the unique tyrosine residue present in both puroindolines is hydrogen-bonded to water. Raman spectra have been recorded in both H_2O and D_2O media, thus providing additional information concerning the accessibility of certain residues to water. We have also observed that puroindoline-a tends to form some aggregates under acidic and high ionic strength conditions. Near-ultraviolet circular dichroism measurements suggest that the tryptophan-rich domain is involved in this aggregate formation. Finally, on the basis of a combined infrared and sequence conformational analysis, we propose a secondary structure assignment for both puroindolines. The results show that puroindolines exhibit a similar folding pattern with plant nonspecific lipid-transfer protein and some amylase-protease inhibitors. These proteins could form a homogeneous structural family of plant proteins involved in the defense against pathogens that are probably derived from a common "helicoidal" protein ancestor.

Puroindolines are water-soluble basic and cysteine-rich proteins of about 13 kDa that have been isolated from wheat endosperm using Triton X-114 phase partitioning (Blochet et al., 1991, 1993). Two isoforms named puroindoline-a and puroindoline-b have been purified and characterized. They exhibit more than 50% homology in their amino acid sequence (Blochet et al., 1991; Gautier et al., 1994). Puroindoline-a, the first characterized isoform, contains a unique tryptophan-rich domain (WRWWKWWK) which is at the origin of the name of this protein (from the greek puros for wheat and indoline for the indole ring of tryptophan). This sequence is partly truncated in puroindoline-b (WPTK-WWK). The folding pattern is stabilized by five disulfide bridges.

These proteins are synthesized as preproteins. The higher molecular weight precursor contains a signal peptide and both extra-small sequences at the N- and C-terminal extremities of the protein that are cleaved in the mature protein (Gautier et al., 1994). This complex maturation of puroindolines is probably important for cell routing and expression of their biological function. The function of puroindolines *in vivo*

is still unknown but their capability to inhibit fungal growth, *in vitro*, suggests that they could play a role in the defense mechanism of wheat seeds against pathogens (Marion et al., 1994). For example, a synergistic inhibitory effect against fungal growth has been observed when puroindolines are mixed with other wheat antimicrobial low molecular weight basic and cysteine-rich proteins, purothionins (Marion et al., 1994). Preliminary results using polyclonal antibodies showed that puroindolines are located in the aleurone layer at the periphery of the endosperm, a location compatible with the protection of the seed (Dubreil et al., 1994).

The tight binding of polar lipids to puroindolines (Wilde et al., 1993; Husband et al., 1995), as also observed for thionins (Bohlmann & Apel, 1991), could be responsible for their membratoxic effects on fungal pathogens. This lipid binding and the unique surface properties of puroindolines make these proteins attractive for many food and chemical applications. Puroindolines exhibit good foaming properties but are especially efficient to prevent destabilization of protein foams by lipids, a delicate problem in many food and chemical formulations (Wilde et al., 1993; Clark et al., 1994; Husband et al., 1995). The secondary structure of puroindolines has not yet been determined experimentally except in the preliminary comparison of their three-dimensional structure with that of a wheat nonspecific lipid-transfer protein (Marion et al., 1994). In order to understand the basis of their surface activity and the lipid binding properties of puroindolines, it is important to study puroindolines under different physiological conditions.

Spectroscopic techniques like infrared, Raman, and circular dichroism spectroscopies are powerful methods for the investigation of the conformation of proteins and allow the quantitative analysis of their secondary structure content in aqueous solutions (Arrondo et al., 1993; Byler & Susi, 1986; Dousseau & Pézolet, 1990; Goormaghtigh et al., 1994a−c; Surewicz & Mantsch, 1988; Williams, 1986; Yang et al., 1986). Raman spectroscopy, as well as near-ultraviolet circular dichroism, further provides information on the conformation of disulfide bridges and on the environment of aromatic residues like tyrosine, tryptophan, and phenylalanine. It is well-established that aromatic and basic residues are often involved in toxicity of different peptides (Evans et al., 1989; Menez et al., 1990; Blondelle et al., 1993). The fact that puroindoline-a exists in both membrane-bound and soluble form (Leguernevé, 1992) is an indicator of the toxin role of this protein (Lakey et al., 1994).

In the present study, the conformation of puroindolines has been studied by infrared and Raman spectroscopies in order to determine their secondary structure content and the environment of certain residues. In conjunction with spectroscopic analysis, predictive methods developed by Garnier, Osguthorpe, and Robson, (GOR;[1] Garnier et al., 1978), Holley−Karplus (1989), and Gascuel and Golmard (1988) have been used to assign the location of secondary structure elements with a better accuracy once the overall content of the secondary structure of the protein is experimentally established. In addition, we have observed that, in acidic conditions and in high salt concentration, puroindoline-a has the propensity to form large aggregates. Near-ultraviolet circular dichroism has also been used to further characterize the aggregate state of puroindolines. The results obtained suggest that the tryptophan-rich domain is involved in the formation of large aggregates.

MATERIALS AND METHODS

Sample Preparation. Puroindolines were purified from wheat seeds according to the method described previously by Blochet et al. (1993) and by Wilde et al. (1993). In addition, in order to remove salt contamination from puroindolines, solutions were centrifuged on an Amicon 3000 filter at 7000g for 1 h. Centrifugations were first done with 150 mM NaCl and then with pure distilled water. Puroindolines were finally lyophilized. Solutions of puroindolines were prepared in water at a concentration range of 7−10% by weight. The pH of the solutions was measured with a microelectrode (Microelectrodes Inc., Bedford, NH). The reduced form of puroindolines was obtained by adding dithiothreitol to the solution at a concentration 4-fold higher than that of the cysteine residues. For experiments done in heavy water, puroindolines were first hydrated in an excess of D_2O (0.4% in weight of protein) for a few hours and then lyophilized. Deuterated proteins were hydrated in heavy water just before their spectra were recorded.

Infrared Spectroscopy: Secondary Structure Determination. Aqueous protein solutions were studied using a

temperature-controlled homemade close cell composed of two CaF_2 windows. The cell was fitted with a 6-μm Mylar spacer in order to allow a constant thickness and a better subtraction of the water contribution from the protein spectra (Dousseau et al., 1989). Infrared spectra were recorded on a Bomem DA3-02 FTIR spectrophotometer equipped with a narrow-band MCT detector. A total of 1000 scans was recorded at a resolution of 2 cm^{-1}. Data manipulations were performed with Spectra Calc (Galactic Industries Corp., Salem, NH). Evaluation of the secondary structure content of the proteins from their infrared spectra was achieved using the method of Dousseau and Pézolet (1990). This method is based on the comparison, using partial least-squares analysis, of the amide I and II infrared bands of a protein of unknown structure with those of a set reference proteins of known three-dimensional structure. The main advantage of this method is that it does not rely on band assignments.

Infrared Spectroscopy: Difference Spectra. FTIR spectra of deuterated puroindolines were recorded on a Nicolet Magna 550 spectrometer equipped with a narrow-band mercury−cadmium−telluride detector. Spectra were recorded at 2-cm^{-1} resolution using 500 scans. The difference spectra in the amide I region were all calculated using the spectrum recorded at 5 °C as a reference spectrum. All spectra were normalized between 1600 and 1700 cm^{-1} before subtraction in order to account for any variation of sample thickness.

Raman Spectroscopy. Samples for Raman spectroscopy were transferred into glass capillary tubes (1.8-mm inside diameter) and placed in a thermoelectrically regulated sample holder. Raman spectra were obtained with a Spex Model 1400 double monochromator. A multichanel CCD9000 system from Photometric Ltd. (Tucson, AZ) with an EEV CCD-05-X detector composed of 1152 × 298 pixels, was used as described elsewhere (Savoie et al., 1994). Spectra were composed of 1152 data points covering a spectral region of *ca.* 2000 cm^{-1} recorded with a diffraction gratings of 300 grooves/mm. The Raman spectra were excited with the 514.5-nm line of an argon ion laser (Spectra Physics Model 2020). The laser power at the sample was between 75 and 100 mW. For puroindoline-a in water solution, 10 exposures of 120 s were collected and averaged, whereas for puroindoline-b, 60 exposures of 60 s were used. Raman spectra of both purindolines, in heavy water solution, were obtained using 60 exposures of 60 s.

For proteins in water solution, the spectrum of the buffer was subtracted from that of the protein until the resulting spectrum was linear between 1730 and 1800 cm^{-1} (Williams, 1986). All spectra were then corrected for the fluorescence background with a spline function, smoothed with a Savitski−Golay seven-point function, and finally, normalized using the 1450-cm^{-1} band due to the methylene bending mode as an internal standard.

Light Scattering. Light scattering was measured with the Raman system. The intensity of the light scattering was followed with the multichannel detector at the edge of the Rayleigh line. Samples were cooled by increment of 1 °C followed by an equilibrium period of 2 min. After the equilibrium period, the scattering intensity was measured. The concentration of puroindoline-a was 7−10% by weight of protein.

Near-Ultraviolet Circular Dichroism. Near-ultraviolet circular dichroism spectra (250−350 nm) were recorded with
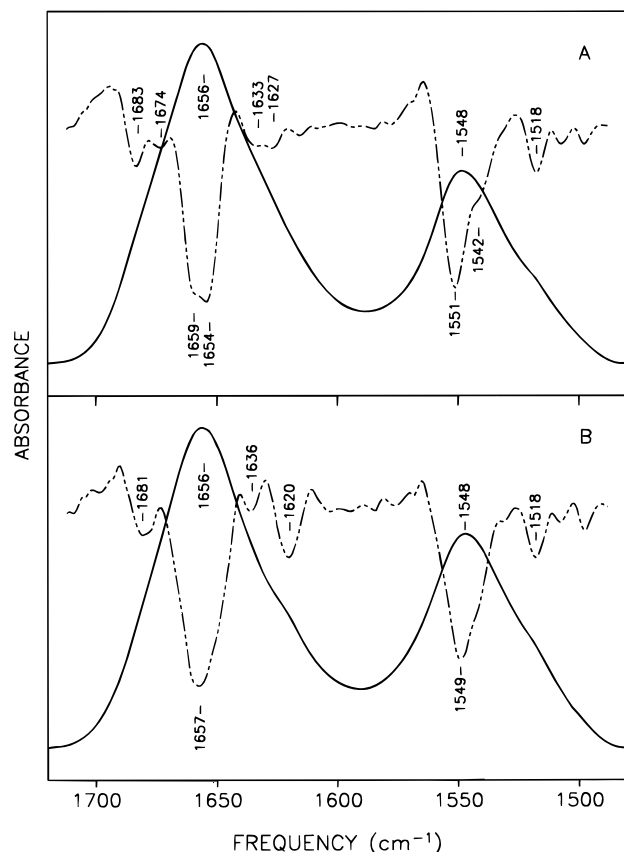
FIGURE 1: Infrared spectra at 20 °C in the amide I and amide II regions of (A) native puroindoline-a and (B) puroindoline-b in H$_2$O, 150 mM NaCl, at pH 7. The solid curves represent the original spectra while the dashed curves are associated with the second derivative (15 pts) of the spectra.

a Jobin-Yvon CD6 spectropolarimeter. Protein solutions were prepared at a concentration of 1 mg/mL in 300 mM NaCl and their pH values were adjusted with either diluted HCl or NaOH solution. CD spectra were measured in a high-quality quartz optical cell of 1 mm path length, and data were expressed as molar ellipticity per residue in degrees centimeter^2 per decimole.

Sequence Analysis. Alignment of protein sequences was carried out with CLUSTAL program from the PC-GENE software based on the multiple sequence described by Higgins and Sharp (1988) and using the Dayhoff mutation data matrix, MDM-78 (Schwartz & Dayhoff, 1978). Secondary structure assignments were done by combining three predictive methods: the Garnier, Osguthorpe, and Robson method (GOR; Garnier et al., 1978), the Gascuel and Golmard basic statistical method (GGBS; Gascuel & Golmard, 1988) using the corresponding programs of the PC-GENE software, and the neural network method of Holley–Karplus (1989) using the CHARMm software. The Holley–Karplus method (HK) was implemented within Quanta as a translated neural net.

RESULTS

Infrared Measurements. Infrared spectra of proteins between 1500 and 1700 cm^{-1} are characterized by two major bands associated with the amide I and II vibrations. Since the position and the shape of these bands are sensitive to the conformation adopted by proteins, they are useful for the evaluation of their secondary structure content. Figure

Table 1: Secondary Structure Contents of Puroindoline-a and -b Determined by Infrared Spectroscopy[a]

structure	α-helix (%)	β-sheet (%)	unordered (%)
Puroindoline-a			
native protein, pH 4	36	27	37
native protein, pH 7	29	30	41
native protein, pH 10	34	27	38
reduced protein, pH 7	9	43	45
Puroindoline-b			
native protein, pH 4	40	25	34
native protein, pH 7	32	29	41
native protein, pH 10	29	30	41
reduced protein, pH 7	14	40	45

[a] The method of Dousseau and Pézolet (1990) was used (see Materials and Methods for details).

1 shows the infrared spectra in this spectral region of puroindoline-a (Figure 1A) and puroindoline-b (Figure 1B) at pH 7. Contribution of the water bending vibration at 1650 cm^{-1} was subtracted from these spectra according to the method of Dousseau et al. (1989). The two major bands, observed at 1656 and 1547 cm^{-1}, are assigned to the amide I and amide II vibrations, respectively. The amide I band at 1656 cm^{-1} is mainly due to the α-helical and unordered structures (Dong et al., 1990; Arrondo et al., 1993; Goormaghtigh et al., 1994a,c).

Band narrowing techniques, like Fourier deconvolution or second derivative, are efficient to decompose the amide I band into its overlapping components. As seen in Figure 1, the second derivative of the amide I band of both puroindolines is composed of approximately four to six components. The two unresolved components at 1654 and 1659 cm^{-1} are assigned to the α-helical and unordered conformations (Dong et al., 1990; Arrondo et al., 1993; Goormaghtigh et al., 1994a,c). The frequency of the amide I band associated with the unordered and α-helical structures is still the object of some controversy. For example, some authors have suggested that, in H$_2$O, the lower component is assigned to the α-helix (*ca.* 1653 cm^{-1}) while the higher component (*ca.* 1656–1660 cm^{-1}) is associated with the unordered structure (Arrondo et al., 1993). On the other hand, Dong et al. (1990) have proposed the inverse for the assignment of these two bands. Weaker bands at 1674 and 1683 cm^{-1} are attributed to turns and β-sheets, respectively (Pézolet et al., 1992; Subirade et al., 1994), whereas bands between 1627 and 1636 cm^{-1} are characteristic of amide groups involved in extended β-sheets (Subirade et al., 1994). For puroindoline-b, an additional feature is observed at 1620 cm^{-1}. This component, is assigned to β-sheets involving stronger hydrogen bonding (i.e., intra- or intermolecular interactions; Arrondo et al., 1988; Clark et al., 1981).

Even though the amide II region is not as well documented as the amide I region, it also provides valuable information on the secondary structure of proteins. Puroindoline-a and -b exhibit a strong band at 1550 cm^{-1} and a shoulder at *ca.* 1518 cm^{-1}. These two bands are usually attributed to the α-helical structure, although tyrosine side chains may also absorb near 1518 cm^{-1} (Goormaghtigh et al., 1994a,c). In order to quantify the secondary structure content of puroindolines, infrared spectra of these proteins have been analyzed with the method of Dousseau and Pézolet (1990). As seen in Table 1, at pH 7, both puroindolines display a similar secondary structure content with approximately 30% α-he-
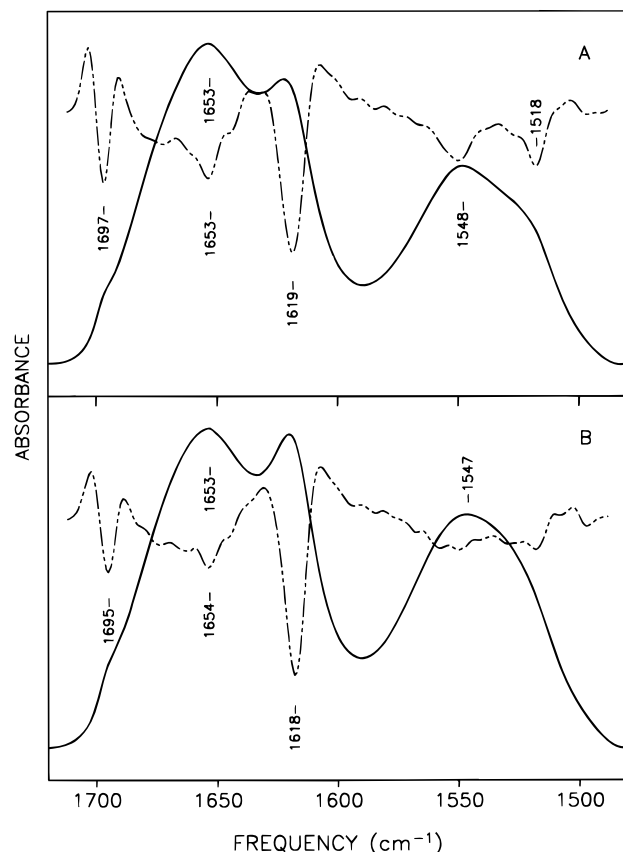
FIGURE 2: Infrared spectra at 20 °C in the amide I and amide II regions of reduced (A) puroindoline-a and (B) puroindoline-b in H₂O, 150 mM NaCl, at pH 7. The solid curves represent the original spectra while the dashed curves are associated with the second derivative (15 pts) of the spectra.
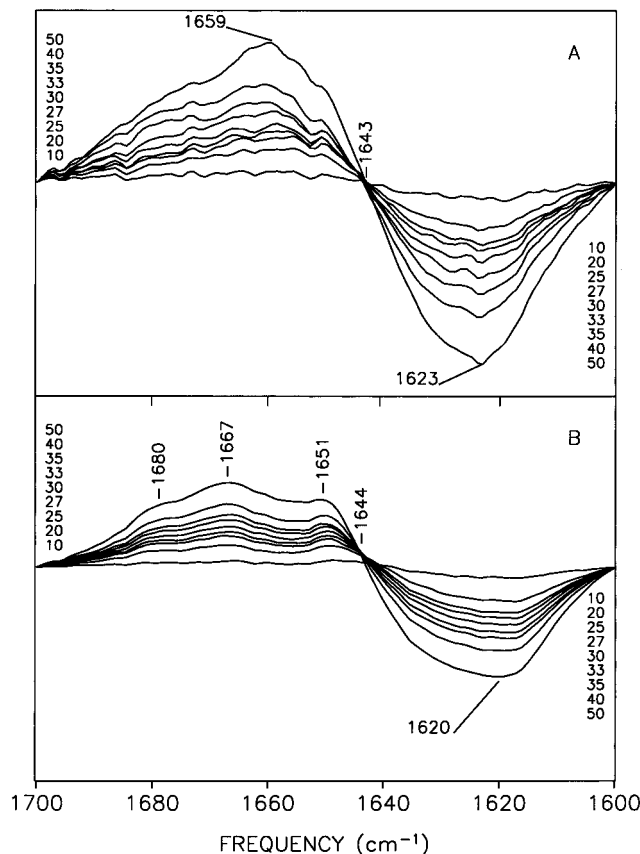

FIGURE 3: Difference infrared spectra relative to the 5 °C spectrum for (A) puroindoline-a and (B) puroindoline-b at different temperatures (as indicated in the corners of the figure). Puroindolines were in solution in D₂O at pD 4 and 300 mM NaCl. Spectra were normalized before subtraction (see the Materials and Methods section).

lices, 30% β-sheets, and 40% of the conformation in an irregular structure or composed of turns.

In order to investigate the role of the disulfide bridges on the stability of puroindolines, infrared spectra of reduced puroindolines were recorded. After reduction, puroindolines tend to form viscous gels. Figure 2 shows that the disruption of the disulfide bridges induces major changes in the infrared spectra. The amide I band is characterized by a major component at 1618–1619 cm⁻¹ assigned to the presence of intermolecular β-sheets since this band has been observed for proteins in an aggregated state (Clark et al., 1981). The observed shoulder at 1695–1697 cm⁻¹ is characteristic of the high-frequency component of the antiparallel β-sheets (Arrondo et al., 1993). The simultaneous appearance of these two components suggests that the β-sheets are antiparallel, as observed for the gluten proteins (Popineau et al., 1994). As illustrated in Table 1, the reduction of the disulfide bonds of puroindolines at pH 7 leads to a decrease of the α-helix content by about 20% and to a raise of the β-sheet content by approximately 15%.

The degree of protonation of side-chain residues can also affect native protein structure. Therefore, the study of the pH-inducted changes of conformation provides valuable information regarding the role of side-chain residues in the stability of the native protein structure. Infrared spectroscopy shows that the secondary structure of puroindolines is sensitive to pH. At pH 4, for both proteins, the α-helix content is about 8% higher than at pH 7. This increase in the α-helix content is observed at the expense of both the

unordered and β-sheet structures. Upon increasing the pH from 7 to 10, the α-helix content of puroindoline-a increases by about 5% at the expense of the unordered and β-sheet structures, while for puroindoline-b, the secondary structure remains unchanged. Therefore, the secondary structure of puroindolines is quite sensitive to both the ionization state of the side chains and to the presence of disulfide bridges.

Under some conditions, puroindolines tend to form aggregates. For example, at pH 4, at high salt concentration (300 mM NaCl), and at low temperature, puroindoline-a solutions have a "milky" appearance associated with the formation of large protein aggregates. This behavior has only been observed for puroindoline-a. In order to investigate the conformational changes associated with the formation of aggregates, difference infrared spectra relative to the 5 °C spectrum have been recorded at different temperatures for puroindolines in solution in D₂O. Difference spectroscopy is an efficient method to detect small differences between conformational states. As illustrated in Figure 3 for puroindoline-a, as the temperature increases, the component at *ca.* 1620 cm⁻¹ (associated with the low-frequency β-sheets) decrease at the expense of the band at 1660 cm⁻¹ (associated with the α-helical structure). As seen in Figure 3, the structural change associated with the increase of temperature is gradual rather than cooperative. However, the isosbestic points at 1643 cm⁻¹ clearly establish that there is a two-state equilibrium between the two forms of the protein. Similar, but weaker, difference spectra were also
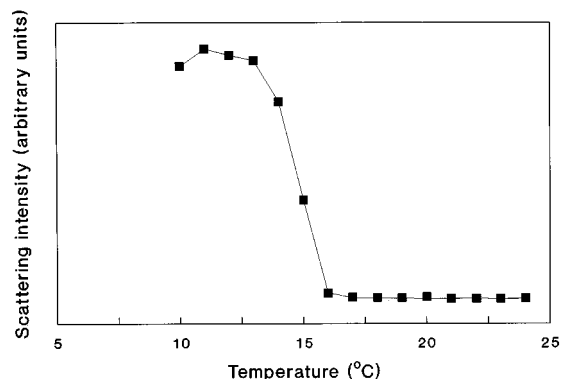
FIGURE 4: Effect of temperature on the Rayleigh light scattering intensity of puroindoline-a. Puroindoline-a was in solution in H_2O at pH 4 in 300 mM NaCl.
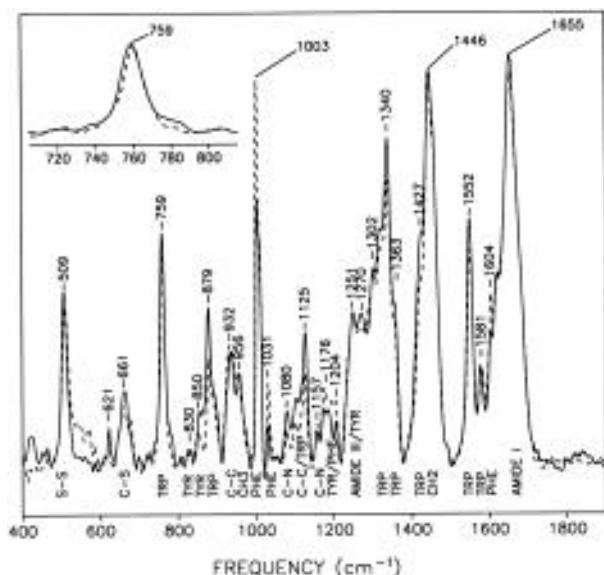

FIGURE 5: Raman spectra of puroindoline-a (solid line) and puroindoline-b (dashed line) at pH 4 in solution in H_2O, 150 mM NaCl, at 20 °C. The assignment of the strongest bands, presented in the bottom of the figure, has been made according to Degrazia et al. (1990), Miura et al. (1988), Tu (1982), and Twardowski (1978).

obtained for puroindoline-b even if this protein does not have the same propensity to form large aggregates as puroindoline-a. Difference spectra in the amide I region were reproducible, even if the observed structural changes are smaller than 5% in the best case.

Light Scattering. As described in the Materials and Methods section, light scattering has been used to characterized the formation of large aggregates in solution of puroindolines. Figure 4 shows the effect of the temperature on the light scattering of puroindoline-a solution. At low temperature, puroindoline-a is in a gel state, and therefore, the scattering intensity is higher. In NaCl solution, the transition occurred at 15 °C and is quite cooperative. This light-scattering property of puroindoline-a solution was not observed for puroindoline-b.

Raman Measurement. Raman spectra were recorded in both H_2O and D_2O in order to analyze any difference in the water accessibility of certain residues. Figures 5 and 6 show Raman spectra of puroindoline-a and -b in solution in H_2O and D_2O, respectively. The assignment of several Raman bands is also shown in these figures. Spectra of both puroindolines are quite similar, thus confirming that these
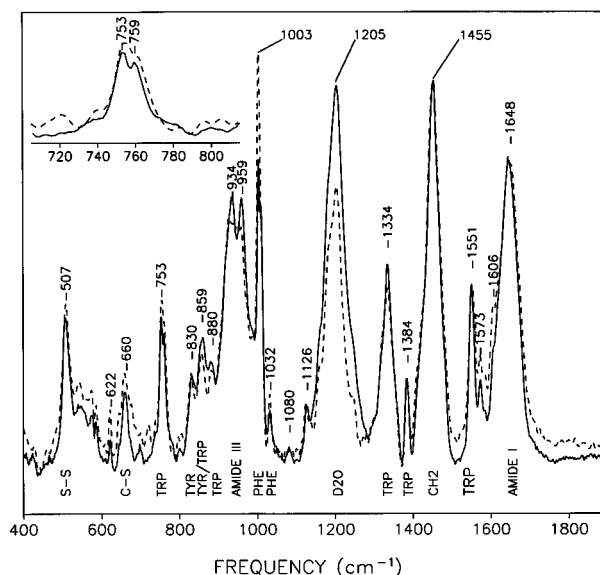

FIGURE 6: Raman spectra of puroindoline-a (solid line) and puroindoline-b (dashed line) at pD 4 in solution in D_2O, 150 mM NaCl, at 20 °C. The assignment of the strongest bands, presented in the bottom of the figure, has been made according to Lord Yu (1970), Tu (1982), and Twardowski (1978).

proteins have a homologous structure. It was not possible to obtain good quality Raman spectra for solutions at pD higher than 4.

The Raman amide I band of puroindoline-a and -b is centered at 1655 cm^{-1} in H_2O and at 1648 cm^{-1} in D_2O, showing that the secondary structure of these proteins is composed of a significant amount of α-helices (Tu, 1982), in agreement with the infrared results. Three major components are observed in the amide III region at 1250, 1270, and 1300 cm^{-1}. In D_2O (Figure 6), these three bands are shifted down in the 930−950-cm^{-1} region thus confirming their assignment to amide III bands. The two components at 1270 and 1300 cm^{-1} are assigned to the α-helical conformation since it has been observed in the Raman spectra of intact muscle fibers (Pézolet et al., 1978, 1980) and of the muscle protein myosin (Carew et al., 1975). The component at 1250 cm^{-1} is assigned to the unordered structure (Tu, 1982). As shown in Figure 5, puroindolines exhibit a band near 930 cm^{-1}, which arises from the skeletal C−C stretching vibration. This band is also an indicator of the presence of α-helices (Pézolet et al., 1980; Clark et al., 1981; Tu, 1982).

The two bands at 830 and 850 cm^{-1} are assigned to the single tyrosine residue of puroindolines. Siamwiza et al. (1975) have shown that this doublet is due to the Fermi resonance between the ring symmetric stretching vibration and the overtone of the C−C and C−O stretching vibrations. It is well-known that the Raman intensity ratio I_{850}/I_{830} is an indicator of the tyrosine environment (Siamwiza et al., 1975). For a high ratio ($I_{850}/I_{830} = 2.5$), the hydroxyl group of the tyrosine acts like an acceptor of strong hydrogen bonds. For a low ratio ($I_{850}/I_{830} = 0.3$), the hydroxyl group is a donor of strong hydrogen bonds. In the case of an intermediate ratio, the hydroxyl group is both donor and acceptor of moderate hydrogen bonds, with water molecules for example. In the case of puroindolines, quantitative evaluation of this ratio was difficult as an intense tryptophan band at 880 cm^{-1} overlaps with the higher component of the tyrosine doublet.

Qualitatively, the ratio I_{850}/I_{830} is higher than 1, suggesting that the tyrosine hydroxyl group is exposed to water molecules.

The presence of disulfide bonds in puroindolines is clearly revealed by the strong band at 509 cm^{-1} due to the S—S stretching vibration. Sugeta et al. (1973) have shown that the frequency of this band is sensitive to the conformation of the C—C—S—S—C—C sequence. Bands at 510, 525, and 540 cm^{-1} are characteristic of the *gauche—gauche—gauche, gauche—gauche—trans,* and *trans—gauche—trans* conformation of the C—C—S—S—C—C sequence, respectively. Since there is only a single and symmetric band at 509 cm^{-1} for both puroindolines, it appears that all the S—S linkages are in the *gauche—gauche—gauche* conformation.

Puroindoline-a and -b contain five and four tryptophan residues, respectively, that give rise to several Raman bands at 760, 880, 1014, 1340, 1363, 1552, and 1582 cm^{-1} characteristic of the indole ring vibration (Tu, 1982). Among these bands, those appearing at 1363 and 880 cm^{-1} are often correlated to the environment of the indole side chain. A sharp intense band at *ca.* 1360 cm^{-1} is an indication of a hydrophobic environment for the tryptophan side chains (Miura et al., 1988). In the case of puroindoline, the absence of a definite peak at 1360 cm^{-1} suggests that the tryptophan-rich domain of these proteins is partly accessible to water. The frequency of the 880-cm^{-1} band allows the evaluation of the strength of hydrogen bonding at the N_1H position of the indole ring. Strong hydrogen bonds lead to a decrease of the frequency of this band (Miura et al., 1988). For puroindolines, the tryptophan band appears at 879 cm^{-1}, indicating that the NH groups of several tryptophan residues are involved in weak hydrogen bonds (Miura et al., 1988).

In D_2O, the 879-cm^{-1} band is shifted to *ca.* 859 cm^{-1} due to deuteration of the NH group but does not completely disappear, suggesting partial deuteration of the indole rings. Therefore, only some tryptophan residues appear to be accessible to the solvent. Similarly, the indole ring-breathing vibration at 760 cm^{-1} in H_2O (Figure 5, inset) is partly shifted to 753 cm^{-1} in D_2O (Figure 6, inset), showing that several tryptophan residues are not accessible to deuteration. Takeuchi and Harada (1986) have observed and calculated a similar isotopic effect for the case of model compounds. The tryptophan band at *ca.* 1429 cm^{-1}, often used in kinetics studies (Miura et al., 1988), is due to a mixed mode of the $N_1C_2C_3$ symmetric stretching, N_1H bending, and benzene CH bending vibrations. This band is downshifted at 1384 cm^{-1} upon deuteration. Figure 6 shows that the intensity of the 1384-cm^{-1} band is the same for both puroindoline-a and -b, suggesting that the same number of tryptophan residues are accessible to deuteration for the two isoforms.

Bands characteristic of the phenylalanine residues are observed at 1003, 1031, 1204, and 1064 cm^{-1}. However, none of these bands can be correlated to specific environments of the phenylalanine side chains (Tu, 1982).

Circular Dichroism Measurement. Near-ultraviolet circular dichroism spectroscopy has also been used in order to get more information on the conformation of the tryptophan-rich domain of puroindoline. Aromatic and cysteine residues give rise to dichroic bands in the near-ultraviolet region that are sensitive to the protein conformation and are useful to monitor conformational transitions occurring under different physicochemical conditions (Strickland, 1974; Woody, 1995).
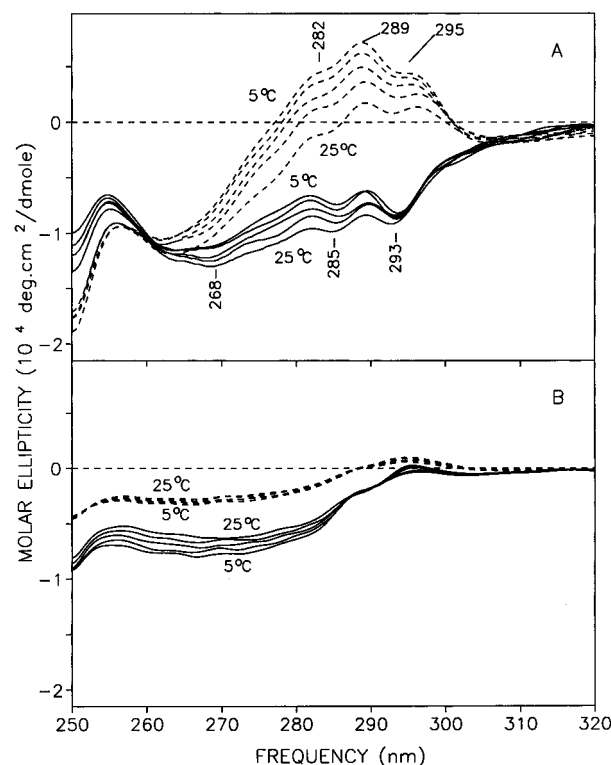
FIGURE 7: Effect of temperature (increments of 5 °C) on the near-ultraviolet circular dichroism spectrum of puroindoline-a (A) and puroindoline-b (B) at pH 4 (solid lines) and pH 7 (dashed lines) in 300 mM NaCl.

Figure 7 shows the effect of temperature on the near-ultraviolet spectrum of puroindoline-a (Figure 7A) and puroindoline-b (Figure 7B). The near-ultraviolet spectrum of puroindoline-a at pH 4 exhibits a minimum at *ca.* 268 nm associated with the disulfide bonds of the protein (Collins & Collier, 1985; Woody, 1995). Other minima, assigned to tryptophan residues, are observed at 285 and 293 nm. For puroindoline-a, increasing the pH from 4 to 7 results in an important change in the dichroism of the tryptophan region (280—300 nm) from a high negative ellipticity to a smaller positive ellipticity. These major variations in the ellipticity of the 280—300-nm region contrast with the slight changes observed in the 250—280-nm region. While increasing the temperature at pH 4 leads to a progressive augmentation of the ellipticity in the 280—300-nm region, it results in a drop of the ellipticity in the same region at pH 7. In the case of puroindoline-b, the ellipticity is lower and much less affected by pH and temperature variations as puroindoline-a. Moreover, increasing the temperature has the opposite effect on the ellipticity of puroindoline-b.

Secondary Structure Prediction. A great structural diversity exists between the low molecular weight and cysteine-rich polypeptide found in cereal seeds. Few three-dimensional (3D) structures are known for these proteins. Recently, Strobl et al. (1995) have determined the 3D structure of a bifunctional α-amylase/trypsin inhibitor from ragi seeds (RBI) by NMR spectroscopy. This protein, which is homologous to the monomeric and homodimeric α-amylase inhibitor from wheat seeds, is comparable in size to puroindolines with about 120 amino acid residues. NMR spectroscopy has shown that the helical content of RBI is similar to that of puroindolines with approximately 33% α-helices. Figure 8 illustrates the sequence alignment of these cereal

```
                                    |——————H1——————|                                              |
       1         10              20             30
1  S V G x T S C I P G M A I P H N P L D S C R W Y V S T R T C G V G P R L A x x x x x x x x x x x x x x x T
       1          10               20               30                40
2  D V A G G G G A Q Q C P V E x T K L N S C R N Y L x L D R C S T M K D F P V T W R W W K W W K G G C x
       1          10               20               30                40
3  E V G G G G S Q Q C P Q E R P K L S S C K D Y V x M E R C F T M K D F P V T W P T x K W W K G G C E
                    1          10               20
4  x x x x x x x I x D C G H V D S L V R P C L S Y V x x x Q G G P G P S G x x x x x x x x x x x x x x x x x
                                      |——————————H1——————————|
```

```
   |————————H2————————|                                  |————H3————|
          40             50                        60             70
1  Q E M K A R C C R Q L E A I x P A Y x x x x x x x x x x x C R C E A V R I L M D G V V T S S G Q H E G R L
          50             60                        70
2  Q E L L G E C C S R L G Q M P P Q x x x x x x x x x x x C R C N I I Q G S I Q x x x x x x x x x x x G D L
          50             60                           70                              80
3  H E V R E K C C K Q L S Q I A P Q x x x x x x x x x x x C R C D S I R R V I Q x x x x x x x x x x x x G R L
                 30                  40               50                   60
4  x x x x x Q C C D G V K N L H N Q A R S Q S D R Q S A C N C x x L K G I A R G x x x x x G I H N x x x
       |————————H2————————|                          |————————H3————————|
```

```
            |————H4————|
        80            90              100             110               120
1  x L Q D L P G C P R Q V Q R A F A P x K L V T E V E C N L A T I x x x H G G P F C L S L G A G E
      80            90             100              110
2  G x G I F G F Q R D R A S K V I Q E x A K N L P P R C N Q G P P x x x x x x x x x C N I P G T x x x
      80             90              100             110
3  G x G F L G I W R G E V F K Q L Q R x A Q S L P S K C N M G A D x x x x x x x x x C K F P S G x x x
                                  70                  80                 90
4  x L N x x x x x x x x x x x x x E D N A R S I P P K C G V N L P Y T I S L N I D C x S R V x x x x
      |————————————H4————————————|
```

FIGURE 8: Alignment of the primary structure of (1) RBI , (2) puroindoline-a, (3) puroindoline-b, and (4) wheat ns-LTP. Description of the alignment of the multiple sequence has been done as presented in the sequence analysis section of Materials and Methods. The location of the four α-helices (H1−H4) of RBI and the wheat ns-LTP, as determined from the 3D structure of these proteins, is also reported in this figure. Shaded boxes indicate conserved residues that are common to RBI or wheat ns-LTP and one of the puroindolines. The numbering illustrated given for each sequence does not include blanks and is, therefore, specific to each protein.

Table 2: Assignment of the α-Helices for RBI, Wheat ns-LTP, and Puroindoline-a and -b

	RBI				wheat ns-LTP				puroindoline-a				puroindoline-b			
	3D[a]	HK	GGBS[b]	GOR[b]	3D[c]	HK	GGBS[b]	GOR[b]	align	HK	GGBS[d]	GOR[d]	align	HK	GGBS[d]	GOR[d]
H1	18−29				5−18		5−10	1−11	17−28	19−25	15−33	14−30	18−29	21−32	18−30	22−32
H2	37−51	33−48	34−64	35−48	26−36	30−39	30−40	30−40	49−62	45−60		50−57	50−63	49−60	48−61	48−61
H3	58−65	51−63		51−65	45−56	43−55	44−63	47−57	69−76				70−77	73−78	68−73	
H4	87−94	87−97	90−106	92−107	62−68	62−67		62−67	87−100	85−95	85−97	86−97	89−101	87−99	86−98	87−98

[a] Location of the α-helices from NMR spectroscopy (Strobl et al., 1995). [b] Location of the α-helices considering the secondary structure contents given by the 3D structure. [c] Location of the α-helices from NMR spectroscopy (Gincel et al., 1994; Petit et al., 1994). [d] Location of the α-helices considering the secondary structure contents determined by infrared spectroscopy.

inhibitors with the sequence of both puroindoline-a and puroindoline-b. The wheat nonspecific lipid-transfer protein (ns-LTP), another cysteine-rich protein of known 3D structure (Gincel et al., 1994; Petit et al., 1994), also exhibits a similar secondary structure composition with 55% α-helices according to NMR results (Grincel et al., 1994). Although, with 90 amino acid residues, the amino acid sequence of the wheat ns-LTP is shorter than those of puroindolines and RBI, a satisfactory alignment is observed (Figure 8). The polypeptide backbone of both RBI and wheat ns-LTP is composed of four α-helices connected by loops of variable length. The best sequence fit corresponds to the α-helix zones of both RBI and wheat ns-LTP. This homology leads us to propose also the existence of four helices for both puroindolines: residues 17−28 and 18−29 for H1, 49−62 and 50−63 for H2, 69−76 and 70−77 for H3, and 87−100 and 89−101 for H4 for puroindoline-a and puroindoline-b, respectively: (Figures 8 and 9 and Table 2). The sequence alignment does not allow the determination of the probable location of the extended structure for puroindolines. The zone where the β-sheet structure is found in RBI (residues 67−75) does not match with a homologous region of puroindolines as illustrated in Figure 8.

Three secondary structure prediction methods based on the primary sequence of amino acids were used in order to localize with the highest accuracy the secondary structures of puroindolines. The GOR method is an algorithm that determines the propensity of an amino acid to be in an α-helix, an extended structure, a turn, or a coil structure as evaluated from the analysis of proteins of known 3D structures. The conformation of a given residue depends on the influence of eight residues before and eight residues after (Garnier et al., 1978; Garnier & Robson, 1989). The Holley−Karplus method (HK) is based on a neural network that recognized three states: helix, sheet and coil. The neural network has been trained on 48 proteins with known 3D structure and uses a window of 17 residues to determine the secondary structure assignment of the central residue (Holley & Karplus, 1989). The Gascuel and Golmard basic statistical method (GGBS) is a local and residue-by-residue method that determines the most probable conformational state for each amino acid of the protein using data derived from the known three-dimensional structure of 62 proteins (Gascuel & Golmard, 1988). Only GOR and GGBS allow for modification of decision constants or parameters in order to obtain the desired secondary structure content (Garnier &

Robson, 1989; Gascuel & Golmard, 1988) and thus to locate with better accuracy the secondary structure elements along the primary sequence. In the case of puroindolines, the decision constants were thus adjusted to obtain the same secondary structure contents as determined experimentally by infrared spectroscopy at pH 7 (see Table 1).

In order to evaluate the accuracy of these three predictive methods, they have been tested on wheat ns-LTP and RBI, which are proteins of known three-dimensional structure (Table 2). The decision constants and parameters of the GOR and GGBS methods were adjusted in order to obtain the secondary structure contents given by the 3D structures (Strobl et al., 1995; Gincel et al., 1994; Petit et al., 1994). In the case of wheat ns-LTP, only the GOR method can predict with acceptable accuracy the four helices, while for RBI predictive methods give satisfactory results only for the localization of H2 and H4 helices (Table 2). None of the predictive methods used in this work was able to predict the H1 α-helix of RBI (Table 2). These results emphasize the fact that these predictive methods have to be used with caution.

Location of H1, H2, and H4 α-helices in puroindoline-a and -b revealed by the sequence alignments is confirmed by the different predictive methods except for the H2 α-helix of puroindoline-a, which is not predicted by the GGBS method. Most of the methods used in this work partly failed to predict the existence of the H3 helix. The H3 helix is only predicted for puroindoline-b by the GGBS and HK methods although the last method also suggests β-sheet for the same sequence. The α-helix H3 being a very conserved sequence between RBI, wheat ns-LTP, and puroindolines, it is highly probable that an α-helix is formed in this part of the polypeptide.

Concerning other structural elements, the 3D structures of RBI and wheat ns-LTP clearly reveal lower contents of β-sheet or extended structures than those estimated from spectroscopic methods like IR or CD (Strobl et al., 1995; Gincel et al., 1994; Désormeaux et al., 1992; Alagiri & Singh, 1993). The three-dimensional structure of wheat ns-LTP does not reveal the existence of β-sheets and shows only 7% β-sheets in the case of RBI, while IR and CD predicted a β-sheet content of 20−30% for both proteins. The precise reason for this discrepancy between 3D structure obtained by NMR spectroscopy and β-sheet contents estimated by IR and CD spectroscopy is still unknown. It is possible that protein segments that are not observed as β-sheets by NMR spectroscopy give rise to infrared or CD spectra that are similar to the spectral features associated with the β-sheet structure. However, the glycine-rich zone (from approximately residue 79−89) of both puroindolines is systematically predicted as β-sheet by the GOR and HK methods and is located between the H3 and H4 helices as the antiparallel β-sheet found in RBI (Strobl et al., 1995). The tryptophan-rich domain is probably formed by β-turn or unordered structure and could form a loop between helices H1 and H2.

DISCUSSION

The analysis of the amide I and II bands of the infrared spectra of puroindoline-a and -b indicates that the secondary structure of these proteins is very similar and consists of about 30% α-helix, 30% β-sheet, and 40% unordered conformation. The amide I band at 1656 cm^{-1} is assigned

to the α-helix and unordered structures. The spectrum of native puroindoline-b also exhibits a band around 1620 cm^{-1} associated with a characteristic β-sheet structure specific to protein involved in gels or aggregate states (Clark et al., 1981). A similar band at 1620 cm^{-1} has also been observed for concanavalin A (Arrondo et al., 1988) and for native diphtheria toxin (Cabiaux et al., 1989). Nevertheless, our results are partly in disagreement with the structure prediction deduced from far-ultraviolet circular dichroism measurements by Husband et al. (1995). These authors obtained 25% α-helices, 50% β-sheets, and 25% aperiodic structures.

Despite the presence of five disulfide bridges, the secondary structure of both puroindolines is pH-dependent, thus suggesting structural flexibility. Reduction of disulfide bonds leads to a significant loss of solubility and a marked decrease of the α-helix content at the expense of the β-sheet structure. Spectra of reduced puroindolines are characterized by two specific bands at *ca.* 1620 and 1695 cm^{-1} that clearly establish the presence of intermolecular antiparallel β-sheets. Our results demonstrate unambiguously that the disulfide bonds stabilize the α-helical structure in puroindolines and are necessary to maintain the native structure and solubility of these proteins. The S−S stretching vibration at 509 cm^{-1} shows that the five disulfide bonds of puroindoline-a and -b are in a *gauche−gauche−gauche* conformation. It is well-known that this conformation gives relatively short and stable S−S bonds. Similar results have been observed for the nonspecific wheat phospholipid transfer protein (Désormeaux et al., 1992).

Raman results provide valuable information on the environment of the aromatic side chains of puroindolines. Both puroindolines possess one tyrosine residue of conserved position. The Raman doublet associated with this residue shows that the phenolic hydroxyl group of this tyrosine side chain is not bound to a negatively charged carboxylate residue of the protein but is rather hydrogen-bonded to water molecules. Therefore, it seems that the tyrosine side chain is exposed to the aqueous environment. In puroindoline-a tryptophan residues are located in the region between positions 39 and 45 and forms a unique tryptophan-rich domain. Puroindoline-a has one additional tryptophan compared to puroindoline-b and lacks two phenylalanine residues. These differences can be used to confirm the band assignment. For example, bands due to tryptophan residues at 880, 1125, 1340, 1363, 1429, and 1552 cm^{-1} are more intense in the spectrum of puroindoline-a than in that of puroindoline-b. This is not the case for the band at 760 cm^{-1}, as also observed by Miura et al. (1991) for lysozyme. Miura et al. (1991) have established that an increase in the intensity of the 760-cm^{-1} component might be assigned to a weaker hydrophobicity of the tryptophan side chains. Unlike the other tryptophan bands, the component at 760 cm^{-1}, which has the same intensity for the two puroindolines, shows that tryptophan residues of puroindoline-b are in a less hydrophobic environment than those of puroindoline-a. As illustrated in the inset of Figure 6, the splitting of the band at 760 cm^{-1} resulting from the partial deuteration of the indole ring clearly establishes that approximately 50% of the tryptophan residues are deuterated. Therefore, the tryptophan-rich sequence between residues 39 and 45 appears to be partly accessible to the solvent, according to previous results showing that the maximum of fluorescence intensity of puroindoline-a is at about 340 nm (Wilde et al., 1993). It
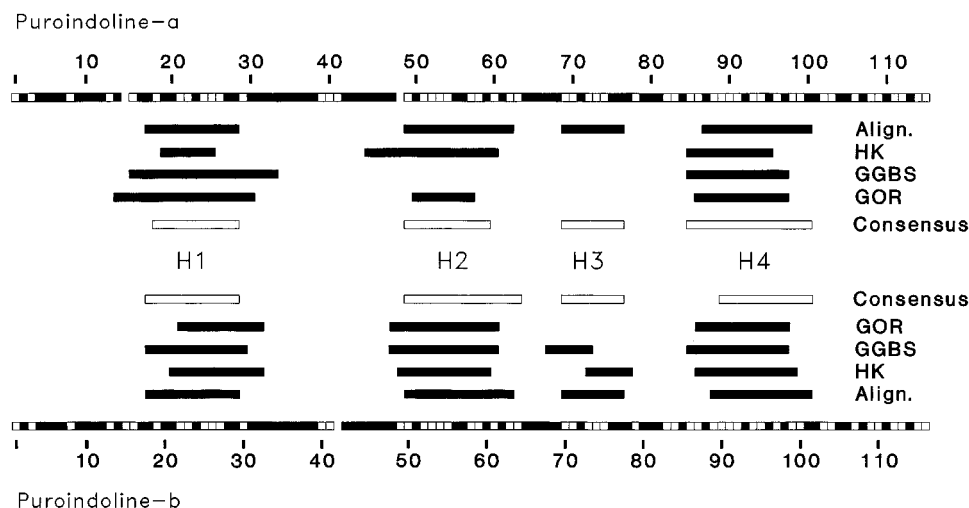
FIGURE 9: Comparison of the predicted α-helices for puroindoline-a and puroindoline-b. Helices were predicted from the sequence homology (Align.) as illustrated in Figure 8 and from the Holley−Karplus method (HK), the Gascuel and Golmard basic statistical method (GGBS), and the Garnier, Osguthorpe, and Robson method (GOR). A sequence consensus is proposed from these methods for both puroindolines. The conserved residues that are common to both puroindolines are indicated in black along the sequence.

has been shown that the maximum of fluorescence intensity ranges from 350 nm for tryptophan residues totally exposed to aqueous solvent to 330 nm when tryptophan residues are buried in a hydrophobic environment (Lakowicz, 1986).

An intriguing difference between puroindoline-a and -b is the propensity of puroindoline-a to form aggregates at low pH and at high salt concentration, a property that resembles the so-called molten globule state (Kuwajima, 1989; Goto & Fink, 1989). A molten globule state could, therefore, explain why puroindoline-a, which is a water-soluble protein, can bind polar lipids, as observed, for example, with α-lactalbumin in the same conformational state (Kim & Kim, 1986). Preliminary infrared and Raman results on the aggregate state of puroindoline-a suggest no important change of its secondary structure. Even though the gel formation that occurs for puroindoline-a at low temperature, resulting in the formation of large macroscopic aggregates that scattered visible light, is cooperative (as illustrated in Figure 4), the temperature dependence of the secondary structure of puroindoline-a, observed by infrared spectroscopy (Figure 3), is rather gradual. Moreover, a similar variation in the secondary structure of puroindoline-b is observed despite the fact that this protein has not the propensity to form large aggregates at the macroscopic level. These results show that secondary structure changes observed by infrared spectroscopy are probably dissociated from the gel-forming property of puroindoline-a. Similarly, it has been observed that, for β-lactamase, the secondary structure is unaffected by the aggregation state (Goto & Fink, 1989). An aggregated state is usually the result of the exposure of hydrophobic residues of the protein, favoring in this way protein−protein interactions. At low pH, aspartic and glutamic acid residues are probably protonated, thus resulting in electrostatic repulsions between charged basic groups and leading to a destabilization of the native structure of the protein. At high salt concentration, the presence of counterions around the basic charged groups reduces these repulsions and probably favors a folding pattern.

To our knowledge, the molten globule state of puroindoline-a has not been previously reported. Therefore, near-ultraviolet circular dichroism measurements have been made in order to detect the existence of a molten globule state of

puroindoline-a. The molten globule state, mainly characterized by a loss of asymmetry in aromatic residues, gives flat spectra between 250 and 300 nm (Mitchinson & Pain, 1985). This is not the case for puroindoline-a, for which dichroic spectra are observed both at acidic and neutral pH in the 5−25 °C range. However, the concentration used for near-ultraviolet CD is considerably lower (0.1%) than that used for vibrational spectroscopy (7−10%). It cannot be excluded that, at the concentration used for vibrational spectroscopy, protein−protein interactions can stimulate the formation of this particular conformational state. However, near-ultraviolet CD measurements were also carried out at 10 mg/mL that gave strictly identical results to those obtained at 1 mg/mL (results not shown).

Interestingly, in the case of puroindoline-a, the tryptophan-rich region exhibits high ellipticity in the near-ultraviolet region, suggesting electric dipole−dipole coupling due to a close packing and relatively rigid structure of tryptophan residues (Strickland, 1974). The change of the value and the sign of the molar ellipticity when the pH is reduced from 7 to 4 could be due to a close intramolecular packing of the tryptophan residues resulting in a conformational transition like from loop to helix. Another hypothesis could be based on intermolecular interactions between monomers of puroindoline-a, where the tryptophan-rich domain would be directly involved in close contact between monomers without any conformational change. Such large variations in the near-ultraviolet CD spectra were not observed for puroindoline-b, although both puroindolines exhibit an increment in their α-helix content when the pH is lowered from 7 to 4 (see Table 1). It is therefore probable that large variations in the ellipticity could be due to intermolecular interaction between monomers involving the tryptophan-rich sequence of puroindoline-a. In addition, our infrared results show that the proportion of intermolecular β-sheets is more important for puroindoline-b. Therefore, we think that the b-isoform has a higher tendency to form small autoassociation structures that could prevent aggregation on a larger scale.

The tryptophan-rich domain has been suspected to play a role in the oligomerization of aerolysin, a membranotoxin secreted by a Gram-negative bacterium (Buckley, 1992). Ahmad et al. (1995) have observed that indolicidin, a

tryptophan-rich peptide, has the property to self-associate. Interestingly for this peptide, the self-association state coincides with an *in vitro* hemolytic activity. Similarly, we have previously observed that the affinity of puroindoline-a for the micellar phospholipid lysophosphatidylcholine is higher than that of puroindoline-b (Husband et al., 1995).

Changes in the near-ultraviolet circular dichroism spectra are less pronounced in the spectral region corresponding to cysteine and phenylalanine residues, suggesting that the regions of puroindoline where these residues are located are not directly involved in the aggregation phenomenon.

The combination of the three predictive methods (GOR, GGBS, and HK) used in this study with sequence alignment with homologous proteins of known 3D structure allows a consensus assignment for the location of the α-helices in puroindolines. Moreover, the location of α-helices can be determined with better accuracy if the homology between both puroindolines is considered, especially for the location of the H3 helix, as illustrated in Figure 9. A sequence consensus in the case of puroindolines can be found by considering the following factors: the sequence homology between puroindolines, RBI, and ns-LTP, also the location of the α-helices deduced by the predictive methods, the helix-breaker character of glycine and proline residues, and finally the consideration of a similar content in α-helices estimated by infrared spectroscopy. As shown on Figure 9, the four α-helices of puroindoline-a and -b could have the following locations, respectively: residues 18−28 and 18−29 for H1, 49−59 and 50−64 for H2, 69−76 and 70−77 for H3, and 85−100 and 90−101 for H4. These four α-helices represent approximately 40% of the overall protein structure despite the fact that we imposed a content of *ca.* 30% in α-helices with the GOR and GGBS method. This difference can be explained by the fact that these two predictive methods have not been able to locate adequately the third α-helix, except for puroindoline-b where a small α-helix was predicted by the GGBS method. All four predictive methods reveal the existence of helices H1 and H4 for both puroindolines and H2 for puroindoline-b. Nevertheless, some variation concerning the length of these α-helices is observed depending on the predictive methods used. Table 2 also shows that these predictive methods were not able to predict unambiguously the location of the α-helices in homologous proteins of known 3D structure.

The secondary structure assignment shown in Figure 9 for both puroindolines suggests that loops link helices and allow the protein to fold in a compact 3D structure stabilized by disulfide bonds. In this regard, the tryptophan-rich domain (residues 39−45) corresponds to an important extension of the first loops of wheat ns-LTP (Gincel et al., 1994) and of RBI that contain protease inhibitory activity (Strobl et al., 1995).

Finally, these results suggest that puroindolines could be a member of a structurally related family of proteins, including lipid transfer proteins and amylase inhibitors. Most of these proteins are believed to play a role in the defense mechanism of plants against pests and microbial pathogens (Molina et al., 1993; Marion et al., 1994). From an evolutionary point of view, it is tempting to suggest that these proteins are derived from a common helicoidal protein ancestor where their specific activity, enzyme inhibition, and membrane binding, for example, proceed from essential residues mainly located in loops. This has generated from a common mold a wide range of proteins with different inhibitory activities adapted to the different plant predators present in the environment. Such a situation resembles that observed for immunoglobulins, which are composed of a conserved domain, preserving the protein structure, and a highly variable domain involved in specific recognition of antigens.

REFERENCES

Ahmad, I., Perkins, W., Lupan, D., Selsted, M., & Janoff, A. (1995) *Biochim. Biophys. Acta 1237*, 109−114.

Alagiri, S., & Singh, T. (1993) *Biochim. Biophys. Acta 1203*, 77−84.

Arrondo, J. L. R., Young, N. M., & Mantsch, H. H. (1988) *Biochim. Biophys. Acta 952*, 261−286.

Arrondo, J. L. R., Muga, A., Castresana, J., & Goni, F. M. (1993) *Prog. Biophys. Mol. Biol. 59*, 23−56.

Blochet, J. E. (1991) Thesis, Université de Nantes, France.

Blochet, J. E., Chevalier, C., Forest, E., Pebay-Peyroula, E., Gautier, M. F., Joudrier, P., Pézolet, M., & Marion, D. (1993) *FEBS Lett. 329*, 336−340.

Blondelle, S. E., Simpkins, L. R., Pérez-Payá, E., & Houghten, R. A. (1993) *Biochim. Biophys. Acta 1202*, 331−336.

Bohlmann, H., & Apel, K. (1991) *Annu. Rev. Plant Physiol. Plant Mol. Biol. 42*, 227−240.

Buckley, J. T. (1992) *FEBS Lett. 307*, 30−33.

Byler, M. D., & Susi, H. (1986) *Biopolymers 25*, 469−487.

Cabiaux, V., Goormaghtigh, E., Wattiez, R., Falmagne, P., & Ruysschaert, J. M. (1989) *Biochimie 71*, 153−158.

Carew, E. B., Asher, I. M., & Stanley, H. E. (1975) *Science 188*, 933−936.

Clark, A., Saunderson, D., & Sugget, A. (1981) *Int. J. Pept. Protein Res. 17*, 353−364.

Clark, D. C., Wilde, P. J., & Marion, D. (1994) *J. Inst. Brew. 100*, 23−25.

Collins, C. M., & Collier, J. R. (1985) *Biochim. Biophys. Acta 828*, 138−143.

Degrazia, H., Harman, J. G., Tan, G.-S., & Wartell, R. M. (1990) *Biochemistry 29*, 3557−3562.

Désormeaux, A., Blochet, J. E., Pézolet, M., & Marion, D. (1992) *Biochim. Biophys. Acta 1121*, 137−152.

Dong, A., Huang, P., & Caughey, W. S. (1990) *Biochemistry 29*, 3303−3308.

Dousseau, F., & Pézolet, M. (1990) *Biochemistry 29*, 8771−8779.

Dousseau, F., Therrien, M., & Pézolet, M. (1989) *Appl. Spectrosc. 43*, 538−542.

Dubreil, L. Quillien, L., Legoux, M.-A., Compoint, J.-P., & Marion, D. (1994) in *Proceedings of the wheat kernel proteins—molecular and functional aspects*, pp 331−333, Universita della Tuscia, C. N. R., Italy.

Evans, J., Wang, Y., Shaw, K.-P., & Vernon, L., P. (1989) *Proc. Natl. Acad. Sci. U.S.A. 86*, 5849−5853.

Garnier, J., & Robson, B. (1989) in *Prediction of protein structure and the principles of protein conformation* (Fasman, G., Ed.), pp 1−99, Plenum Press, New York and London.

Garnier, J., Osguthorpe, D. J., & Robson, B. (1978) *J. Mol. Biol. 120*, 97−120.

Gascuel, O., & Golmard, J. L. (1988) *Comput. Appl. Biosci. 4*, 357−365.

Gautier, M.-F., Aleman, M.-E., Guirao, A., Marion, D., & Joudrier, P. (1994) *Plant Mol. Biol. 25*, 43−57.

Gincel, E., Simorre, J.-P., Caille, A., Marion, D., Ptak, M., & Vovelle, F. (1994) *Eur. J. Biochem. 226*, 413−422.

Goormaghtigh, E., Cabiaux, V., & Ruysschaert, J.-M. (1994a) in *Subcellular Biochemistry* (Hilderson, H. J., & Ralston, G. B., Eds.) Vol. 23, pp 329−362, Plenum Press, New York.

Goormaghtigh, E., Cabiaux, V., & Ruysschaert, J.-M. (1994b) in *Subcellular Biochemistry* (Hilderson, H. J., & Ralston, G. B., Eds.) Vol. 23, pp 363−403, Plenum Press, New York.

Goormaghtigh, E., Cabiaux, V., & Ruysschaert, J.-M. (1994c) in *Subcellular Biochemistry* (Hilderson, H. J., & Ralston, G. B., Eds.) Vol. 23, pp 405−450, Plenum Press, New York.

Goto, Y., & Fink, A. (1989) *Biochemistry 28*, 945−952.

Higgins, D. G., & Sharp, P. M. (1988) *Gene 73*, 237−244.

Holley, H. L., & Karplus, M. (1989) *Proc. Natl. Acad. Sci. U.S.A. 86*, 152−156.

Husband, F., Wilde, P. J., Marion, D., & Clark, D. C. (1995) in *Food Macromolecules and colloids* (Lorient, D., & Dickinson, E., Eds.) pp 285−296, Royal Society of Chemistry, London.

Kim, J., & Kim, H. (1986) *Biochemistry 25*, 7867−7874.

Kuwajima, K. (1989) *Proteins: Struct., Funct., Genet. 6*, 87−103.

Lakey, J. H., Parker, M. W., Gonzalez-Manas, J. M., Duché, D., Vriend, G., Baty, D., & Pattus, F. (1994) *Eur. J. Biochem. 220*, 155−163.

Lakowicz, J. R. (1986) *Methods Enzymol. 131*, 518−567.

Leguernevé, C. (1992) Thesis, Université de Nantes, France.

Lord, R. C., & Yu, N.-T. (1970) *J. Mol. Biol. 50*, 509−524.

Marion, D., Gautier, M.-F., Joudrier, P., Ptak, M., Pézolet, M., Forest, M., Clark, D. C., & Broekaert, W. (1994) in *Proceeding of the wheat kernel proteins−molecular and functional aspects*, pp 175−180, Universita della Tuscia, C. N. R., Italy.

Menez, A., Gatineau, E., Roumestantd, C., Harvey, A., Mouawad, L., Gilquin, B., & Toma, F. (1990) *Biochimie 72*, 575−588.

Mitchinson, C., & Pain, R. H. (1985) *J. Mol. Biol. 184*, 331−342.

Miura, T., Takeuchi, H., & Harada, I. (1988) *Biochemistry 27*, 88−94.

Miura, T., Takeuchi, H., & Harada, I. (1991) *Biochemistry 30*, 6074−6080.

Molina, A., Segura, A., & Garcia-Olmedo, F. (1993) *FEBS Lett. 316*, 119−122.

Petit, M. C., Sodano, P., Marion, D., & Ptak, M. (1994) *Eur. J. Biochem. 222*, 1047−1054.

Pézolet, M., Pigeon-Gosselin, M., & Caillé, J. P. (1978) *Biochim. Biophys. Acta 533*, 263−269.

Pézolet, M., Pigeon-Gosselin, M., Nadeau, J., & Caillé, J.-P. (1980) *Biophys. J. 31*, 1−8.

Pézolet, M., Bonenfant, S., Dousseau, F., & Popineau, Y. (1992) *FEBS Lett. 299*, 247−250.

Popineau, Y., Bonenfant, S., Cornec, M., & Pézolet, M. (1994) *J. Cereal Sci. 20*, 15−22.

Savoie, R., Pézolet, M., Dallaire, S., & Simard, C. (1994) *Can. J. Appl. Spectrosc. 39*, 164−173.

Schwartz, R. M., & Dayhoff, M. O. (1978) in *Atlas of Protein Sequence and Structure,* Vol. 5, Suppl. 3, pp 353−358, National Biomedical Research Foundation, Washington, DC.

Siamwiza, M., Lord, R., Chen, M., Takamatsu, T., Harada, I., Matsuwra, H., & Shimanouchi, T. (1975) *Biochemistry 14*, 4870−4876.

Strickland, E. H. (1974) *Crit. Rev. Biochem. 2*, 113−175.

Strobl, S., Mühlahn, P., Bernstein, R., Wiltscheck, R., Maskos, K., Wunderlich, M., Huber, R., Glockshuber, & Holak, T. (1995) *Biochemistry 34*, 8281−8293.

Subirade, M., Gueguen, J., & Pézolet, M. (1994) *Biochim. Biophys. Acta 1205*, 239−247.

Sugeta, H., Go, A., & Miyazawa, T. (1973) *Bull. Chem. Soc. Jpn. 46*, 3407−3411.

Surewicz, W. K., & Mantsch, H. H. (1988) *Biochim. Biophys. Acta 952*, 115−130.

Takeuchi, H., & Harada, I. (1986) *Spectrochim. Acta 42A*, 1069−1078.

Tu, A., (1982) in *Raman spectroscopy in biology: Principles and applications*, John Wiley & Sons, New York and Toronto.

Twardowski, J. (1978) *Biopolymers 17*, 181−190.

Wilde, P. J., Clark, D. C., & Marion, D. (1993) *J. Agric. Food Chem. 41*, 1570−1576.

Williams, R. W. (1986) *Methods Enzymol. 130*, 311−331.

Woody, R. W. (1995) *Methods Enzymol. 246*, 34−71.

Yang, J. T., Wu, C.-S., Martinez, H. M. (1986) *Methods Enzymol. 130*, 208−269.